ISSN 0735-2727, Radioelectronics and Communications Systems, 2019, Vol. 62, No. 12, pp. 649–659. © Allerton Press, Inc., 2019.
Russian Text © The Author(s), 2019, published in Izvestiya Vysshikh Uchebnykh Zavedenii, Radioelektronika, 2019, Vol. 62, No. 12, pp. 759–771.

Efficient CFO Estimation and Compensation Approach in OFDMA for Uplink Mobile WiMax

M. Lakshmanan[1*], P. S. Mallick[2], L. Nityanandan[3], M. Sai Krishna[4]
[1]*Galgotias College of Engineering and Technology, Greater Noida, India*
[2]*VIT University, Vellore, India*
[3]*Pondicherry Engineering College, Pillaichavadi, India*
[4]*Virtusa Consulting Services Limited, Pune, India*
**ORCID: 0000-0002-1924-3112, e-mail: tmlakshmanan@gmail.com*

Received March 23, 2015
Revised January 3, 2019
Accepted November 4, 2019

Abstract—Synchronization is a complex task in uplink Orthogonal Frequency Division Multiple Access (OFDMA) for Mobile WiMax as each user presents different Carrier Frequency Offsets (CFO). Synchronization begins with the CFO estimation and followed by the compensation of residual CFO present in the received signal. This paper deals with various techniques in time and frequency domains to compensate the effect of CFO on the received signal for different estimation techniques. SImple time domain MultiUser Interference Cancellation (SIMUIC) performs in time domain. It employs delays in the compensation of CFO while synchronizing the last user. Decorrelation Successive Interference Cancellation (DC-SC) and Integrated Estimation and Compensation (IEC) perform in frequency domain for the compensation of CFO. These approaches are more complex for Inter-Carrier Interference (ICI) cancellation. In this paper, we propose a new efficient CFO compensation technique in frequency domain for different estimation methods. This technique is a modified version of IEC for reducing the CFO effect on the received signal with lesser computations. Simulation results show that the modified IEC performs better than SIMUIC, DC-SC and IEC for different estimation methods.

DOI: 10.3103/S0735272719120057

1. INTRODUCTION

Orthogonal Frequency Division Multiple Access (OFDMA) is one of the multiple access schemes for future wireless broadband and high-speed networks. It provides high data rate and meets the required Quality of Service (QoS).

Mobile WiMax [1] employs OFDMA in uplink for achieving high data rate in wireless broadband network. In OFDMA, the total available subcarriers are grouped and each group assigns to a particular active user with one of the subcarrier assignment strategies. OFDMA is more prone to Carrier Frequency Offsets (CFO) owing to fluctuations in the frequencies at transmitter or receiver and the Doppler shift. Since each user has different CFO, synchronization becomes more difficult in OFDMA [2–5].

CFO leads to two types of interferences, namely, MultiUser Interference (MUI) and Inter Symbol Interference (ISI). MUI occurs due to the interference from subcarriers of another user. Inter-Carrier Interference (ICI) occurs due to the interference between their own subcarriers. Hence, synchronization is more critical in uplink OFDMA for mobile WiMax. It includes the CFO estimation for available active users in the system, and estimated CFOs [6, 7] compensate the effect of the appropriate offsets. An important task lies in the fact that there is a need to design a synchronization method, which can produce a good performance.

This paper deals with various techniques to compensate CFO effect on the received signal in time and frequency domains. SImple time domain MultiUser Interference Cancellation (SIMUIC) method operates in time domain. The synchronization of the last user is performed after all other users are demodulated. Hence, it takes larger time delay to compensate CFO during synchronization of the last user.

Decorrelation Successive Interference Cancellation (DC-SC) and Integrated Estimation and Compensation (IEC) techniques [8] are the frequency domain approaches designed to compensate the CFO effect on the received signal. In DC-SC, the decorrelation method reduces ICI and the successive interference cancellation method reduces MUI.

The main issue in DC-SC is that there will be an error in the estimated CFO that is called residual frequency offset (RFO). IEC is an iterative [9] approach of DC-SC where the compensated output is fed back to the estimation stage for correcting the RFO. DC-SC and IEC have a more complex method for ICI cancellation. This technique is a modified version of IEC, which reduces the number of computations without any degradation of performance.

The remaining part of the paper is structured as follows. The next section includes the system model and discusses the effect of CFO on received signal. The third section explains the Data Aided Phase Incremental Technique (DA-PIT) method for estimating CFO, the time and frequency domain approaches for compensation. The proposed compensation approach is explained in the fourth section. The fifth section discusses the simulation results and section 6 presents the conclusions.

2. SYSTEM MODEL

In this paper, we consider K users and N subcarriers in OFDMA for uplink Mobile WiMax system. Here, we use block subcarrier assignment strategy to allocate groups of subcarriers to active users.

Each active user knows the subcarrier assignment strategy at the base station. The value of N_i is the set of subcarriers allocated to the ith user and there are no common subcarriers between any two different active users such that

$$\bigcup_{i=1}^{k} N_i = \{0,1,2,\ldots,N-1\}. \tag{1}$$

Each active user modulates its own subcarriers with independent and identically distributed symbols bearing information taken from a finite number of constellations. The value of N_g denotes the length of Cyclic Prefix (CP) that appends in front of each symbol for reducing ISI.

At the receiver side, signal $y(n)$ after removing the cyclic prefix, in discrete time domain is represented as

$$y(n) = \sum_{i=1}^{K} \sum_{l=0}^{L-1} x_i(n-l) e^{j2\pi n \varepsilon_i / N} * h_i(l) + w_i(n), \tag{2}$$

where $y(n) = \{y(0), y(1), \ldots, y(N-1)\}$ denotes the received signal, "*" denotes convolution, $h_i(l) = \{h_i(0), h_i(1), h_i(1), \ldots, h_i(L-1)\}$ indicates the impulse response of L-tap multipath channel for the ith active user, $w(n)$ represents the complex white Gaussian noise with variance σ^2, and $\varepsilon_i = \Delta f / f_{\text{sub}}$ denotes the normalized CFO of the ith active user.

We consider the perfect synchronization in time domain and estimates the CFO for the users in uplink. These estimated CFOs are available at receiver side and Discrete Fourier transform (DFT) is performed on received signal $y(n)$ in (2).

The output at the kth subcarrier $Y(k)$ in discrete frequency domain is given as follows:

$$Y(k) = \sum_{i=1}^{K} \sum_{u \in N_i} X_i(u) H_i(u) C(u,k,\varepsilon_i) + W_i(k), \tag{3}$$

where $X_i(u), H_i(u)$, and $W_i(k)$ are the DFTs of $x_i(n)$, $h_i(n)$, and $w_i(n)$, respectively. The var C represents the interference of the uth subcarrier on kth subcarrier due to frequency offset ε_i for the ith active user.

The interference C of the uth subcarrier on the kth subcarrier due to frequency offset ε_i for ith active user, is given as

$$C(u,k,\varepsilon_i) = e^{j\pi(u-k-\varepsilon_i)\frac{N-1}{N}} \frac{\sin(\pi(u-k-\varepsilon_i))}{N \sin\left(\frac{\pi(u-k-\varepsilon_i}{N}\right)}. \tag{4}$$

The DFT of L-tap multipath channel response $h_i(l)$ for the ith active user is $H_i(k)$ and it is given as

$$H_i(k) = \sum_{l=0}^{L-1} h(l) e^{j2\pi lk/N}. \tag{5}$$

Assuming $(k \in N_i)$, the kth subcarrier information for the ith user is written as

$$Y_i(k) = X_i(k)H_i(k)C(u,k,\varepsilon_i) + \sum_{\substack{u \in N_i \\ u \neq k}} X_i(u)H_i(u)C(u,k,\varepsilon_i) + \sum_{\substack{j=1 \\ j \neq i}}^{K} \sum_{u \in N_j} X_j(u)H_j(u)C(u,k,\varepsilon_j) + W_i(k). \tag{6}$$

The first term in (6) $X_i(k)H_i(k)C(u,k,\varepsilon_i)$ represents the desired signal of the ith active user combined with its multipath channel component and the interference C of the uth subcarrier on the kth subcarrier.

The second term $\sum_{\substack{u \in N_i \\ u \neq k}} X_i(u)H_i(u)C(u,k,\varepsilon_i)$ denotes ICI caused due to the interference between their own subcarriers. The third term $\sum_{\substack{j=1 \\ j \neq i}}^{K} \sum_{u \in N_j} X_j(u)H_j(u)C(u,k,\varepsilon_j)$ denotes MUI caused due to the interference from the subcarriers of another user.

3. RELATED WORKS

3.1. CFO Estimation

The active users insert pilot subcarriers in OFDMA symbols repeatedly during the transmission. There is a phase rotation between any two consecutive OFDMA symbols θ_2 due to the frequency offset ε and it is given as

$$\theta_2 = 2\pi \frac{N_s}{N} \varepsilon, \tag{7}$$

where $N_s = N + N_g$.

There is a phase rotation between the first and third OFDMA symbols θ_3 due to the frequency offset ε and it is given as

$$\theta_3 = 2\pi \frac{2N_s}{N} \varepsilon. \tag{8}$$

The phase rotation θ_3 in (8) is twice that of the rotation θ_2 in (7). So, CFO estimation using (8) is more accurate as compared to the estimation using (7). When the CFOs are small, their range using (8) is exactly a half of the range using (7) for estimation. If the CFOs and multipath channel remain uniform for M OFDMA symbols, then the pilot subcarrier is used in the first and Mth OFDMA symbols. It is noted that the same pilot subcarrier information is present in the first and Mth OFDMA symbols at the same location.

3.1.1. Data Aided Phase Incremental Technique (DA-PIT)

Figure 1 depicts the CFO estimation using the Data Aided Phase Incremental Technique (DA-PIT) [10]. It estimates CFO by inserting pilot subcarrier in each data frame. Here, each active user inserts a pilot subcarrier in the first and mth OFDMA symbols of their data frame. The location of the pilot subcarrier is assumed to be available at the receiver.

After performing FFT, the pilot subcarriers are separated from the received data frame. The correlation $C_i(p)$ after FFT [11] at the pth pilot subcarrier is given as

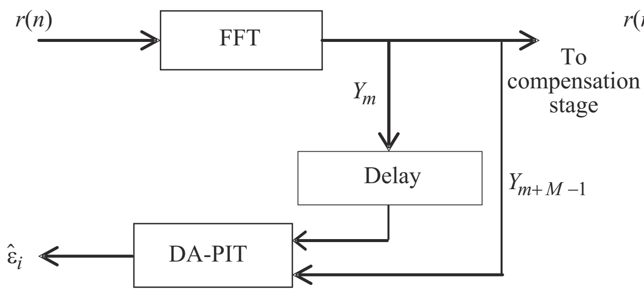

Fig. 1. CFO estimation using DA-PIT.

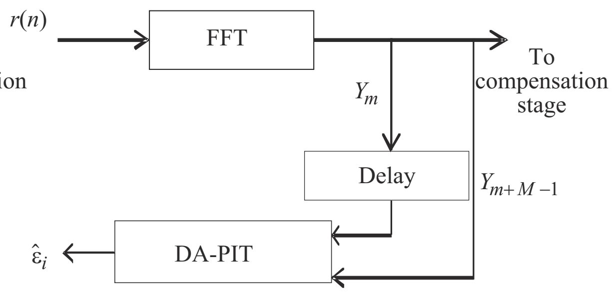

Fig. 2. MDA-PIT.

$$C_i(p) = Y_m^*(p) Y_{m+M-1}(p), \tag{9}$$

where $Y_m(p)$ and $Y_{m+M-1}(p)$ represent the pth pilot subcarrier extracted from the mth and $(m + M - 1)$th OFDMA symbols.

Using (9), CFO, $\hat{\varepsilon}_i$ is estimated as follows:

$$\hat{\varepsilon}_i = \frac{N}{2\pi(N_s)(M-1)} \arg\sum_p C_i(p), \tag{10}$$

where arg(.) denotes the phase shift between the mth and $(m + M - 1)$th OFDMA symbols.

From (10), it is inferred that the required number of computations does not increase with the value of M. The major drawback of DA-PIT is that CFO is estimated once for M OFDMA symbols. It is necessary to estimate CFO for each OFDMA symbol for fast varying channels. DA-PIT estimates CFO when it is identical for M OFDMA symbols.

3.1.2. Modified DA-PIT (MDA-PIT)

Figure 2 depicts the CFO estimation using Modified DA-PIT (MDA-PIT). We consider a quasi-static channel between the mobile station and base station. Here, the channel is static for one OFDMA symbol. This technique estimates CFO by inserting pilot subcarrier in each data frame. Here, each active user inserts a pilot subcarrier in the first and the mth OFDMA symbols of their data frame. The location of the pilot subcarrier is assumed to be available at the receiver.

After performing FFT, the pilot subcarriers are separated from the received data frame. The correlation after FFT, $U(p)$ at the pth pilot subcarrier is given as

$$U(p) = Y_m(p) Y_{m+M-1}^*(p), \tag{11}$$

where $Y_m(p)$ and $Y_{m+M-1}(p)$ represent the pth pilot subcarrier extracted from the mth and $(m + M - 1)$th OFDMA symbols.

Introduce the value

$$V(p) = X_m(p) X_{m+M-1}(p), \tag{12}$$

where $X_m(p)$ and $X_{m+M-1}(p)$ represent the pth pilot subcarrier at the mth and $(m + M - 1)$th OFDMA symbols.

CFO of the first and third OFDMA symbols affects respective OFDMA symbols in the transmitted signal, then

$$e^{j2\pi\hat{\varepsilon}_i \frac{-2N_s}{N}} = \frac{(Y_m(p) Y_{m+M-1}^*(p))}{(X_m(p) X_{m+M-1}(p))}. \tag{13}$$

Using (11) and (12), equation (13) is rewritten as follows:

$$j2\pi\hat{\varepsilon}_i \frac{-2N_s}{N} = \ln\left(\frac{U(p)}{V(p)}\right). \tag{14}$$

From (14), CFO $\hat{\varepsilon}_i$ is estimated as follows:

$$\hat{\varepsilon}_i = \frac{jN\ln\left(\frac{U(p)}{V(p)}\right)}{2\pi(N_s)(M-1)}. \tag{15}$$

3.2. Time Domain Compensation Technique

3.2.1. Simple Time Domain Multiuser Interference Cancellation (SIMUIC)

In the conventional receiver structure using Single FFT, one block of FFT demodulates all active users at same time. Considering the scenario with multiple CFOs, a conventional receiver using Single FFT is not efficient as it demodulates one user at a given time and the remaining users are misaligned. In multiple FFT receiver structure, one OFDMA demodulation block is assigned to each active user so that the CFO effect is compensated independently and individually in time domain.

After compensation, the output of OFDMA demodulator for the ith user is given as

$$Y_i(k) = \mathbf{A}_u \mathbf{F}_N \left(e^{\frac{-k2\varepsilon n}{N}} \right) r(n) = X_i(k) H_i(k)$$

$$+ \sum_{\substack{j=1 \\ j\neq i \\ u\in N_j}}^{K} X_j(u) H_j(u) C_{\varepsilon_j} + W_j(k), \tag{16}$$

where $\mathbf{A}_u$ is the diagonal matrix for selecting the subcarriers of particular user, $\mathbf{F}_N$ is the FFT matrix, the exponent term $\exp(-k2\varepsilon n / N)$ is the time domain frequency offset correction factor and $r(n)$ is the received signal in discrete time domain after removing the cyclic prefix. The diagonal elements of $\mathbf{A}$ are taken as one for the subcarriers of particular user and the remaining elements are taken as zero.

From (16) it is observed that the attenuation and self-interference factors are eliminated for the ith user provided that its CFO value is exactly predicted, while leaving out MUI. A time domain MUI cancellation scheme is used in multiple FFT receiver structure to eliminate MUI. Initially, received signals are sorted in the order of signal strength and the base station processes these signals from the highest to lowest power signal. The time domain approach for cancelling MUI is shown in Fig. 3.

The received signal for the ith user is represented as

$$r_{i,j} = C_{-\varepsilon_i}\left[r(n) - \sum_{p_1=1}^{K} C_{\varepsilon_{p1}} r_{p_1,j} - \sum_{p_2=1}^{K} C_{\varepsilon_{p2}} r_{p_2,j-1} \right], \tag{17}$$

where $r_{i,j}$ represents the feedback from the ith user and the jth iteration and $C_{-\varepsilon_i}$ is the frequency offset correction factor given as $\exp(-k2\varepsilon_i n / N)$. The initial iteration of $r_{i,j}$ is taken as zero.

SIMUIC takes more time delay in the compensation of CFO while synchronizing the last user. This is because SIMUIC processes the last user after the demodulation of the remaining users. So, it does not require the information about the channel, but it requires the correct CFO values of each user for compensation.

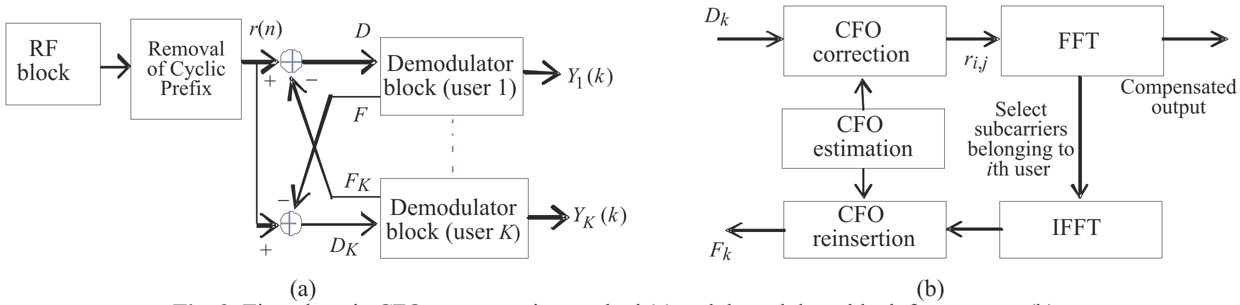

Fig. 3. Time domain CFO compensation method (a) and demodulator block for one user (b).

3.3. Frequency Domain Compensation Techniques

3.3.1. Decorrelation Successive Cancellation (DC-SC)

The received signal is the combination of desired signal, ICI and MUI. DC-SC [12] compensates the effect of ICI and MUI. In DC-SC, the decorrelation method reduces ICI and the successive interference cancellation method reduces MUI.

3.3.1.1. Decorrelation

In decorrelation method, an interference matrix is constructed using the estimated CFO for a group of subcarriers that forms a block. The blocks are arranged in decreasing order of their average powers. Then, the decorrelation is applied to all the subcarriers of the arranged blocks starting from the block having the highest power.

ICI can be compensated from each block by multiplying the received signal with the inverse of interference matrix as follows:

$$\hat{y}_{c_i} = (\hat{C}_i)^{-1} y_{c_i}, \tag{18}$$

where y_{c_i} and $\hat{y}_{c_i}$ are the subcarrier information of the cth block of the ith user with and without ICI, respectively, and $\hat{\mathbf{C}}$ is the interference matrix given as

$$\hat{C}_i = C(u, k, \hat{\varepsilon}_i). \tag{19}$$

ICI and the phase rotation caused to the desired subcarrier due to frequency offset $C(k, k, \hat{\varepsilon}_i)$ are corrected. The subcarrier information $\hat{y}_{c_i}$ obtained from (18) is transmitted with MUI. Then the Successive Interference Cancellation (SC) scheme reduces MUI.

3.3.1.2. Successive Interference Cancellation (SC)

MUI is eliminated from the subcarrier's information without ISI. The interference $\rho_c(k)$ caused by the cth block of the ith user, N_i^c on the kth subcarrier can be reconstructed with the knowledge of estimated CFO and the channel as follows:

$$\rho_c(k) = \sum_{u \in N_i^c} H^i(u) X^i(u) C(u, k, \hat{\varepsilon}_i), \quad k \notin N_i^c, \tag{20}$$

where $H^i(u)X^i(u)$ is the transmitted signal of the cth block, C is the interference of the uth subcarrier on the kth subcarrier with estimated CFO $\hat{\varepsilon}_i$.

Hence, the received output $\hat{Y}(k)$ on the kth subcarrier from the cth block after the removal of MUI is given as

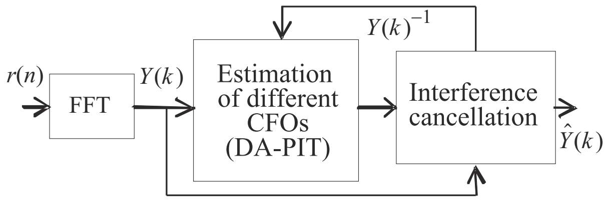

Fig. 4. Integrated CFO estimation and compensation method.

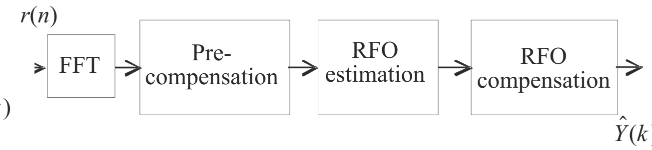

Fig. 5. Modified IEC.

$$\hat{Y}(k) = Y(k) - \rho_c(k), \tag{21}$$

where $Y(k) = \hat{y}_{c_i}$.

SC needs correct data decisions on the demapper for accurate MUI cancellation. This process continues for each subcarrier in all the blocks to eliminate MUI. MUI occurs mostly due to the block of neighbors. Hence, for reducing the computational complexity it is sufficient to eliminate MUI from neighboring blocks rather than from all blocks.

The performance of DC-SC is very much dependent on the accurate estimation of CFO. As estimation is performed in the presence of noise, there exists an offset error RFO. Even a 2% offset introduces a subcarrier phase shift of almost 22°. Therefore, an iterative IEC approach [8, 13] is introduced on DC-SC.

Figure 4 shows the estimation and compensation employed in IEC. In IEC, the compensated output is fed back to the estimation stage for the next iteration. Thus, RFO is estimated at the next iteration and the effect is compensated. The iterative process [14] is repeated to provide a better performance as compared to DC-SC.

The following steps are performed in IEC.

1. Estimate CFO for K active users, i.e. $\hat{\varepsilon}_i$.
2. Update $C_i(u,k,\hat{\varepsilon}_i)$ using (4) with $\hat{\varepsilon}_i$.
3. Compensate ICI and MUI using (18) and (21) using $C_i(u,k,\hat{\varepsilon}_i)$.
4. Return to step 1 using OFDMA symbols corrected in step 3 for the second iteration.

4. MODIFIED IEC

Modified IEC (MIEC) is proposed to reduce ICI and MUI (Fig. 5). In modified IEC, the difference between the CFO of two OFDMA symbols lies within the range of RFO. Hence, the effect of ICI and MUI on the received symbol is precompensated by using the CFO of previous symbol. After precompensation, RFO is estimated and its effect can be compensated at the next iteration, and thus it reduces CFO estimation to one per user per symbol.

The disadvantage of MIEC lies in the fact that if CFO of the ith user for the jth OFDMA symbol is larger than the $(j + 1)$th OFDMA symbol and vice versa, the net CFO will be more than the original CFO. So, the MIEC can be used for every P OFDMA symbols where the slow varying channel is assumed. After performing the MIEC for P OFDMA symbols, the CFO estimation is performed, and this process is repeated for the next consecutive P OFDMA symbols. CFO for the $(j + 1)$th OFDMA symbol is updated by subtracting RFO of the jth CFO from the $(j - 1)$th CFO.

The following are the steps followed in MIEC.

1. Update $C_i(u,k,\hat{\varepsilon}_i)$ using (4) with CFO of previous OFDMA symbol $\hat{\varepsilon}_i$.
2. Compensate ICI and MUI using (18), (21), and $C_i(u,k,\hat{\varepsilon}_i)$ in step 1.
3. Estimate RFO for K active users, i.e. $\hat{\varepsilon}_i$.
4. Compensate ICI and MUI using (18), (21), $C_i(u,k,\hat{\varepsilon}_i)$, and $\hat{\varepsilon}_i$ from step 3.
5. Update CFO for the next OFDMA symbol.

5. RESULTS AND DISCUSSION

Table 1 shows the list of parameters used in the simulation to analyze the Bit Error Rate (BER) performance for various CFO estimation and compensation techniques.

Table 1

Simulation parameter	Value
Number of users (K)	4
Modulation used	16QAM
Number of subcarriers	1024
Type of subcarrier assignment strategy	Block Type
CFO range	{–0.1, 0.1}
Average attenuation in multipath channel	3 dB

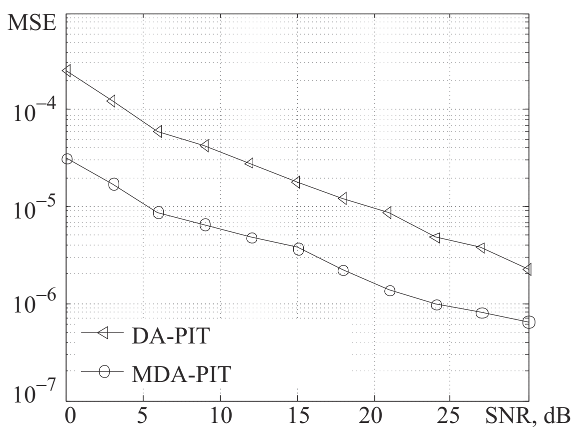

Fig. 6. MSE performance of DA-PIT and MDA-PIT estimations.

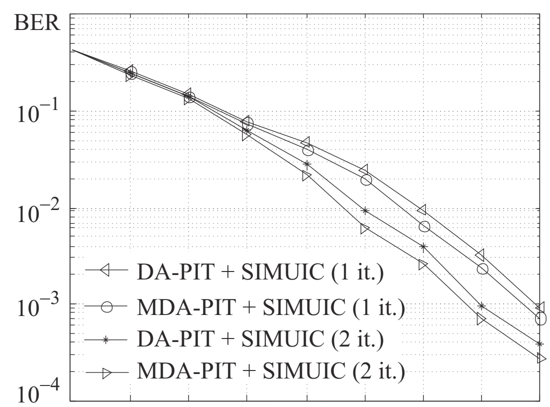

Fig. 7. BER analysis of SIMUIC with DA-PIT and MDA-PIT estimations for one and two iterations.

Figure 6 shows the MSE performance of DA-PIT and MDA-PIT estimations. It is inferred that MDA-PIT has a better Mean Square Error (MSE) as compared to DA-PIT estimation because CFO estimation is more accurate due to a smaller number of computations required in MDA-PIT as compared to DA-PIT estimation.

Figure 7 depicts the BER analysis of SIMUIC compensation with DA-PIT and MDA-PIT estimations for one and two iterations. It can be seen that SIMUIC with MDA-PIT is better than SIMUIC with DA-PIT estimation due to a smaller number of computations. It can be observed that ICI and MUI are reduced when SIMUIC compensation and MDA-PIT employ two iterations.

Figure 8 depicts the BER analysis of DC-SC and IEC compensation methods with DA-PIT and MDA-PIT estimations. It is inferred that IEC DA-PIT and MDA-PIT estimations provide a better BER performance than DC-SC with DA-PIT and MDA-PIT estimations because ICI and MUI are suppressed using the iterative approach in IEC.

Figure 9 shows the BER analysis of MIEC compensated with DA-PIT and MDA-PIT estimations. It is noted that the MIEC with MDA-PIT estimation provides a better BER performance than the MIEC with DA-PIT estimation as the difference between CFO of any two OFDMA symbols lies within the range of RFO. Hence, the effect of ICI and MUI on the received symbol is precompensated using the CFO of previous symbol.

Figure 10 shows the BER analysis of the MIEC, IEC, DC-SC and SIMUIC compensation methods with DA-PIT estimation for single iteration. Figure 11 shows the BER analysis of the MIEC, IEC and DC-SC compensation methods with DA-PIT estimation.

From Figs. 10 and 11 it is inferred that IEC with DA-PIT estimation is better than the modified IEC, DC-SC and SIMUIC with DA-PIT estimation for single iteration because ICI and MUI are suppressed using the iterative approach in IEC without precompensation.

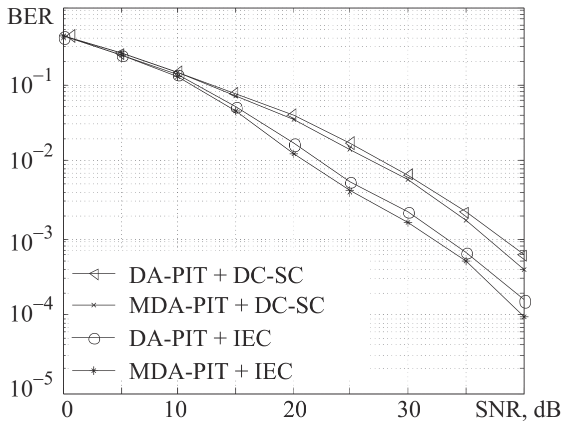

Fig. 8. BER analysis of DC-SC and IEC with DA-PIT and MDA-PIT estimations.

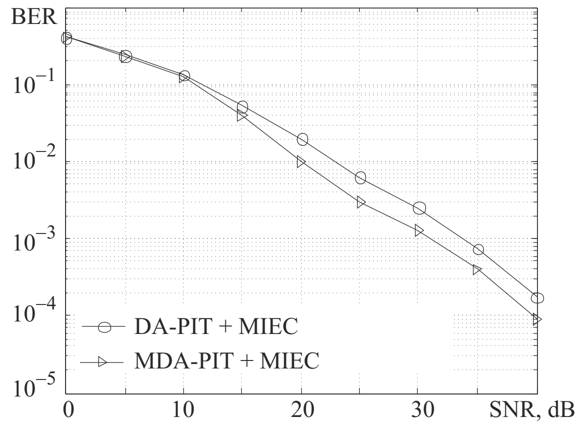

Fig. 9. BER analysis for MIEC with DA-PIT and MDA-PIT estimations.

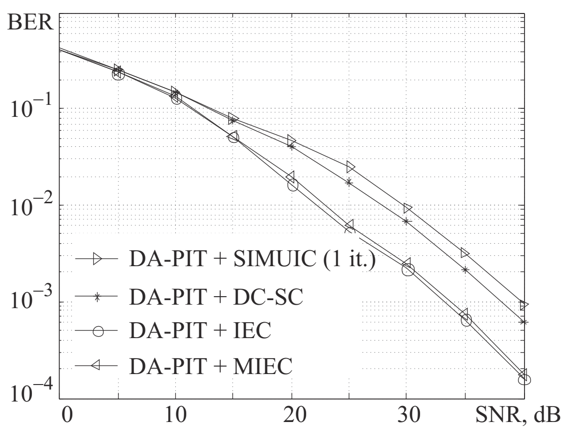

Fig. 10. BER analysis of MIEC, IEC, DC-SC and SIMUIC for single iteration with DA-PIT estimation.

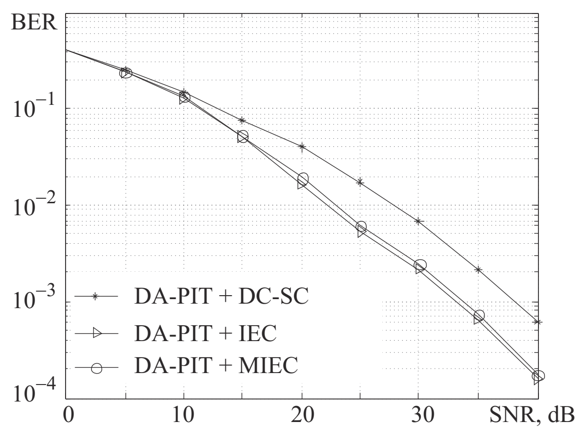

Fig. 11. BER analysis of MIEC, IEC and DC-SC with DA-PIT estimation.

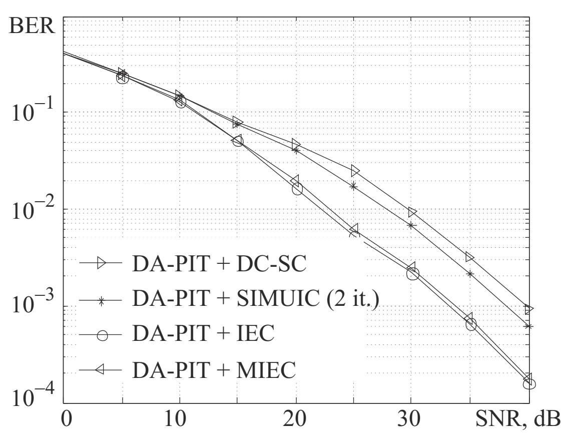

Fig. 12. BER analysis of MIEC, IEC, DC-SC and SIMUIC for two iterations with DA-PIT estimation.

Figure 12 shows the BER analysis of the MIEC, IEC, DC-SC and SIMUIC compensation methods with DA-PIT estimation for two iterations. It can be seen that IEC with DA-PIT estimation is better than the MIEC, DC-SC and SIMUIC with DA-PIT estimation for two iterations because ICI and MUI are suppressed using the iterative approach in IEC without precompensation.

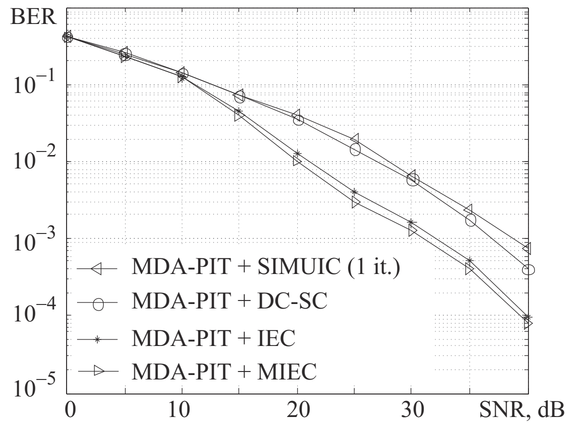

Fig. 13. BER analysis of MIEC, IEC, DC-SC and SIMUIC for single iteration with MDA-PIT estimation.

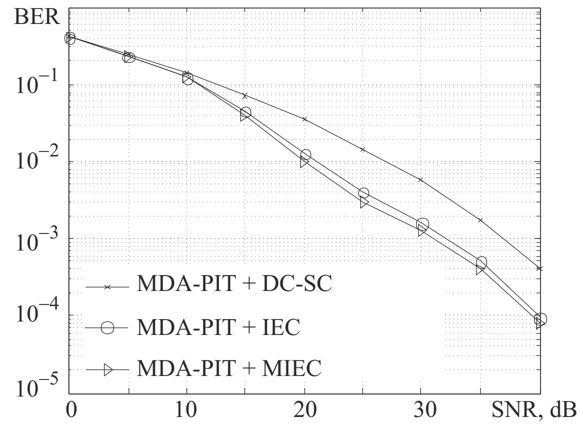

Fig. 14. BER analysis of MIEC, IEC and DC-SC with MDA-PIT estimation.

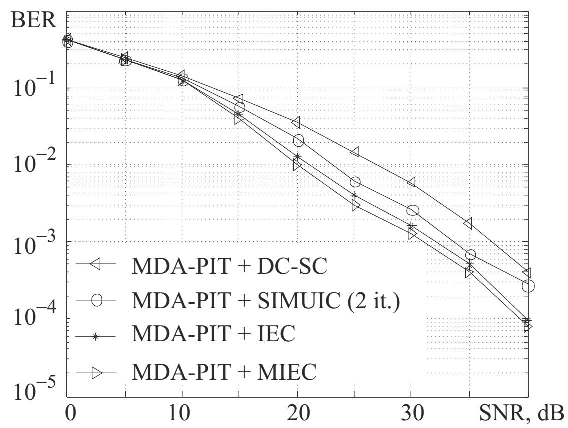

Fig. 15. BER analysis of MIEC, IEC, DC-SC and SIMUIC for two iterations with MDA-PIT estimation.

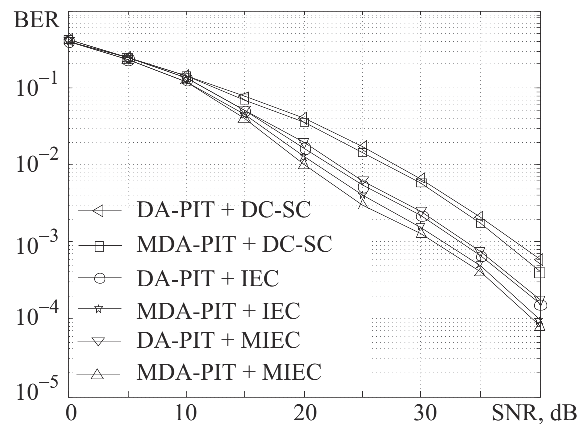

Fig. 16. BER analysis of MIEC, DC-SC and IEC with DA-PIT and MDA-PIT estimations.

Figure 13 shows the BER analysis of the MIEC, IEC, DC-SC and SIMUIC compensation methods with MDA-PIT estimation for single iteration. Figure 14 shows the BER analysis of the MIEC, IEC and DC-SC compensation methods with MDA-PIT estimation.

From Figs. 13 and 14 it can be noted that the modified IEC with MDA-PIT estimation is better than IEC, DC-SC and SIMUIC with MDA-PIT estimation for two iterations. The effect of ICI and MUI on the received symbol is precompensated using the CFO of previous symbol for a reduced amount of computations.

Figure 15 shows the BER analysis of the MIEC, IEC, DC-SC and SIMUIC compensation methods with MDA-PIT estimation for two iterations. It is inferred that the modified IEC with MDA-PIT estimation is more accurate than IEC, DC-SC and SIMUIC with MDA-PIT estimation for two iterations. The effect of ICI and MUI on the received symbol is pre-compensated using the CFO of previous symbol for a smaller number of computations.

Figure 16 shows the BER analysis of the MIEC, IEC and DC-SC compensation methods with DA-PIT and MDA-PIT estimations. It is inferred that the MIEC with MDA-PIT estimation outperforms DC-SC and IEC with DA-PIT and MDA-PIT estimations.

This is due to the efficient suppression of ICI and MUI with a fewer number of computations and due to the fact that the difference between CFO of any two OFDMA symbols lies within the range of RFO. Hence, the effect of ICI and MUI on the received symbol is precompensated using the CFO of previous symbol.

6. CONCLUSIONS

In this paper we propose a new efficient compensation and estimation approach in uplink OFDMA for Mobile WiMax. Simulation results had shown that modified IEC with MDA-PIT estimation outperformed SIMUIC, DC-SC and IEC with DA-PIT and MDA-PIT estimation methods.

Modified IEC had superior performance due to the elimination of ICI and MUI efficiently. It was based on frequency domain approach and required a smaller number of computations to suppress ICI and MUI using slow varying channel concept. The difference between CFO of any two OFDMA symbols fell within the range of RFO. Hence, the effect of ICI and MUI on the received symbol was pre-compensated using the CFO of previous symbol.

CONFLICT OF INTEREST

The authors declare that they have no conflict of interest.

ADDITIONAL INFORMATION

The initial version of this paper in Russian is published in the journal "Izvestiya Vysshikh Uchebnykh Zavedenii. Radioelektronika," ISSN 2307-6011 (Online), ISSN 0021-3470 (Print) on the link http://radio.kpi.ua/article/view/S0021347019120057 with DOI: 10.20535/S0021347019120057.

REFERENCES

1. IEEE standard for Local Area Metropolitan Area Networks, Part 16: Air interface for Fixed and Mobile Broadband Wireless Access Systems - Amendment for Physical and Medium Access Control Layers for Combined Fixed and Mobile Operation in Licensed Bands, IEEE Std. 802.16e (2008). DOI: 10.1109/IEEESTD.2006.99107.
2. S. Barbarossa, M. Pompili, G. Giannakis, "Channel-independent synchronization of orthogonal frequency division multiple access systems," *IEEE J. Selected Areas Commun.* **20**, No. 2, 474 (2002). DOI: 10.1109/49.983375.
3. J. Gonzalez-Bayon, C. Carreras, O. Edfors, "A multistandard frequency offset synchronization scheme for 802.11n, 802.16d, LTE, and DVB-T/H systems," *J. Computer Systems*, *Networks Commun.* **2010**, Article ID 628657, 1 (2010). DOI: 10.1155/2010/628657.
4. M. Morelli, C.-C. J. Kuo, M.-O. Pun, "Synchronization techniques for orthogonal frequency division multiple access (OFDMA): A tutorial review," *Proc. IEEE* **95**, No. 7, 1394 (2007). DOI: 10.1109/JPROC.2007.897979.
5. Z. Cao, U. Tureli, Y.-D. Yao, P. Honan, "Frequency synchronization for generalized OFDMA uplink," *Proc. of IEEE Global Telecommunications Conf.*, 29 Nov.-3 Dec. 2004, Dallas, USA (IEEE, 2004), Vol. 2, pp. 1071-1075. DOI: 10.1109/GLOCOM.2004.1378122.
6. Javier González-Bayón, Angel Fernández-Herrero, Carlos Carreras, "Improved schemes for tracking residual frequency offset in DVB-T systems," *IEEE Trans. Consumer Electronics* **56**, No. 2, 415 (2010). DOI: 10.1109/TCE.2010.5505948.
7. Michael Speth, Stefan Fechtel, Gunnar Fock, Heinrich Meyr, "Optimum receiver design for OFDM-based broadband transmission. II. A case study," *IEEE Trans. Commun.* **49**, No. 4, 571 (2001). DOI: 10.1109/26.917759.
8. Javier Gonzalez-Bayon, Angel Fernandez-Herrero, Carlos Carreras, "A reduced complexity scheme for carrier frequency synchronization in uplink 802.16e OFDMA," *EURASIP J. Advances Signal Processing* **218**, 1 (2012). DOI: 10.1186/1687-6180-2012-218.
9. P. Sun, L. Zhang, "Low complexity pilot aided frequency synchronization for OFDMA uplink transmission," *IEEE Trans. Wireless Commun.* **8**, No. 7, 3758 (2009). DOI: 10.1109/TWC.2009.081005.
10. Y.-H. You, K.-T. Lee, S.-J. Kang, "Pilot-aided frequency offset tracking scheme for OFDM-Based DVB-T," *IEEE Trans. Consum. Electron.* **54**, No. 3, 1053 (2008). DOI: 10.1109/TCE.2008.4637587.
11. S. A. Fechtel, "OFDM carrier and sampling frequency synchronization and its performance on stationary and mobile channels," *IEEE Trans. Consum. Electron.* **46**, No. 3, 438 (2000). DOI: 10.1109/30.883390.
12. T. Yucek, H. Arslan, "Carrier frequency offset compensation with successive cancellation in uplink OFDMA systems," *IEEE Trans. Wireless Commun.* **6**, No. 10, 3546 (2007). DOI: 10.1109/TWC.2007.060273.
13. M. Huang, X. Chen, S. Zhou, J. Wang, "Iterative ICI cancellation algorithm for uplink OFDMA system with carrier-frequency offset," *Proc. of IEEE Veh. Technol. Conf.*, 28 Sept. 2005, Dallas, USA (IEEE, 2005), Vol. 3, pp. 1613-1617. DOI: 10.1109/VETECF.2005.1558214.
14. D. Huang, K. B. Letaief, "An interference-cancellation scheme for carrier frequency offsets correction in OFDMA systems," *IEEE Trans. Commun.* **53**, No. 7, 1155 (2005). DOI: 10.1109/TCOMM.2005.851558.